Metrol. Meas. Syst., Vol. 27 (2020) No. 2, pp. 339–353
DOI: 10.24425/mms.2020.132779

METROLOGY AND MEASUREMENT SYSTEMS
Index 330930, ISSN 0860-8229
www.metrology.wat.edu.pl

TRACKING ERROR ANALYSIS METHOD OF DIGITAL PULSE POWER SUPPLY FOR HEAVY ION ACCELERATOR BASED ON EMD RECONSTRUCTION

Rongkun Wang, Sigun Sun, Bingtao Hu

Huaqiao University, School of Information Science and Engineering, Xiamen 361021, China
(✉ *wangrongkun@hqu.edu.cn*, +86 189 5017 4931, *378962732@qq.com*, *459282014@qq.com*)

Abstract

Assessment of the state of a pulse power supply requires effective and accurate methods to measure and reconstruct the tracking error. This paper proposes a tracking error measurement method for a digital pulse power supply. A de-noising algorithm based on Empirical Mode Decomposition (EMD) is used to analyse the energy of each Intrinsic Mode Function (IMF) component, identify the turning point of energy, and reconstruct the signal to obtain the accurate tracking error. The effectiveness of this EMD method is demonstrated by simulation and actual measurement. Simulation was used to compare the performance of time domain filtering, wavelet threshold de-noising, and the EMD de-noising algorithm. In practical use, the feedback of current on the prototype of the power supply is sampled and analysed as experimental data.

Keywords: pulse power supply, tracking error, EMD, signal reconstruction.

1. Introduction

The *Heavy Ion Research Facility in Lanzhou – Cooler Storage Ring* (HIRFL-CSR) and the *Heavy Ion Medical Machine* (HIMM) have been successfully applied in deep tumor therapy, using a combination mode of cyclotron and synchrotron. The pulse power supply system is the key providing specific current for the magnets to excite the magnetic field required by the accelerator [1]. Both CSR and HIMM function as synchrotrons, and the dipole magnetic field and quadrupole magnetic field synchronously change in one working cycle, which requires that the output of excitation power supplies should also synchronously change [2, 3].

In order to evaluate the performance of pulse power supplies, the tracking error is introduced and it is particularly important to measure and reconstruct this error [4, 5]. Traditional methods include Fourier transform de-noising, Butterworth filtering de-noising, Wavelet transform de-noising [6–8]. Since high-performance digital pulse power supplies provide weak signals that are often overwhelmed by noise, it is difficult to distinguish noise and signals using conventional methods and these methods cause phase difference. Wavelet threshold de-noising algorithm does not produce a phase difference, it is, however, constrained by wavelet base and threshold

parameters selection lacking adaptive ability. *Empirical mode decomposition* (EMD) de-noising algorithm has been widely applied as a new de-noising method with no energy attenuation and phase delay [9]. Furthermore, it has no limitation of basis functions or threshold parameters.

This paper proposes a threshold de-noising method based on EMD, which performs threshold de-noising on the noise-dominated components and superimposes the signal-dominated components to realize signal reconstruction. To achieve good performance of EMD, the extreme point symmetric extension method and a novel method are introduced to solve both boundary problem and mode mixing. Simulation and experiments show that the proposed method facilitates parameter optimization and the control strategy selection for a power supply.

2. Tracking error of pulse power supply

To achieve the synchronous change, it must ensure that the tracking performance of a pulse power supply which describes the ability of the power supply to change its output according to the reference current [10]. Figure 1 shows the typical pulse power supply reference current and tracking error current waveform [2, 4], and the output current is similar to the reference current. The tracking performance is measured by the tracking error index as follows:

$$E_{tr} = I_r - I_{fd} \,. \tag{1}$$

Where E_{tr} is the tracking error of the current, I_r and I_{fd} are the reference current and output current of the power supply. During the rising stage as shown in Fig. 1, I_r rises from the bottom (50 A) to peak (1150 A) in one second [2]. The beam accelerates with the increase of I_{fd}, requiring very high tracking error capability. When I_{fd} tracks I_r to the flat-top stage, the beam is extracted, requiring I_{fd} to remain stable. Due to the different design specifications and pulse waveforms of

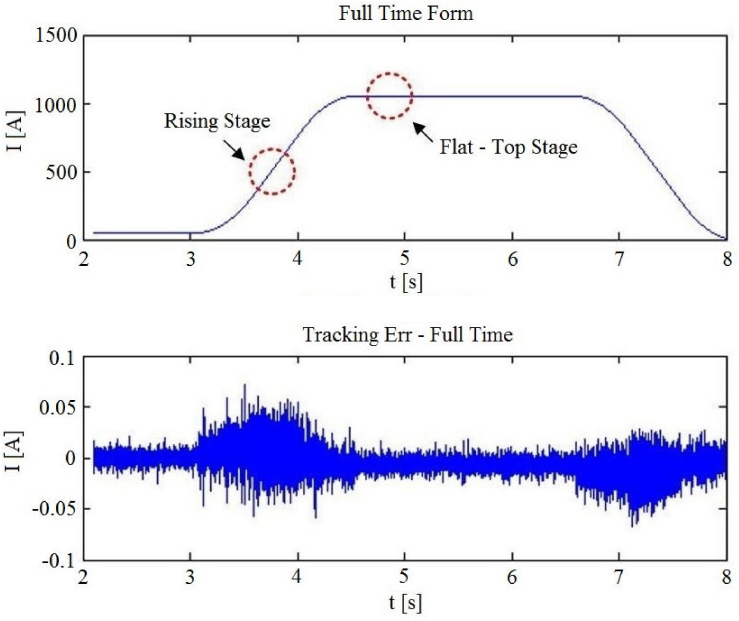

Fig. 1. Reference and tracking error current of a pulse power supply.

Metrol. Meas. Syst., Vol. 27 (2020), No. 2, pp. 339–353
DOI: 10.24425/mms.2020.132779

power supplies, the pulse power supply performance is typically described in terms of the relative tracking error [11]:

$$E'_{tr} = \pm (E_{tr})_{\max} / I_{top} \,. \tag{2}$$

In the formula (2), I_{top}, $(E_{tr})_{\max}$ and E'_{tr} are the output current, maximum tracking error of current and relative tracking error of current, respectively. Where E'_{tr} is relative tracking error in the rising stage, while it is called relative current error in the flat-top stage. E'_{tr} is per unit value which is indicated by p.u. in this paper. Table 1 lists the relative tracking error and relative current error requirements of several typical digital pulse power supplies in HIMM [11].

Table 1. Tracking error indexes of HIMM pulse power supplies.

Power supply type	Quantity	Rated Current (A)	Relative tracking error (rising stage)	Relative current error (flat-top stage)
For Dipolar Magnets	4	1666	$\leq \pm 1.0 \times 10^{-4}$	$\leq \pm 1.0 \times 10^{-5}$
For Quadrupole Magnets	4/8	368/373	$\leq \pm 1.0 \times 10^{-4}$	$\leq \pm 1.0 \times 10^{-5}$
For Correction Coils	8	360	$\leq \pm 5.0 \times 10^{-4}$	$\leq \pm 1.0 \times 10^{-5}$
For Correction Magnets	8	±13.7	$\leq \pm 1.0 \times 10^{-3}$	$\leq \pm 1.0 \times 10^{-3}$
For Sextupole Magnets	7/2	150/305	–	$\leq \pm 1.0 \times 10^{-5}$

3. Acquisition of tracking error

There are two tracking error measurement methods for digital pulse power supplies [10]: the analog and the digital method. As shown in Fig. 2, the digital power supply control part uses dual-loop control with voltage inner loop and current outer loop, and the tracking error measurement part gives the analog and digital methods. The former directly uses the current error and a filter which leads to a phase shift. The latter uses current reference, current feedback and current error to avoid the phase shift caused by the filters in the digital power supply control part. The analog method is more appropriately used for local debugging and provides an

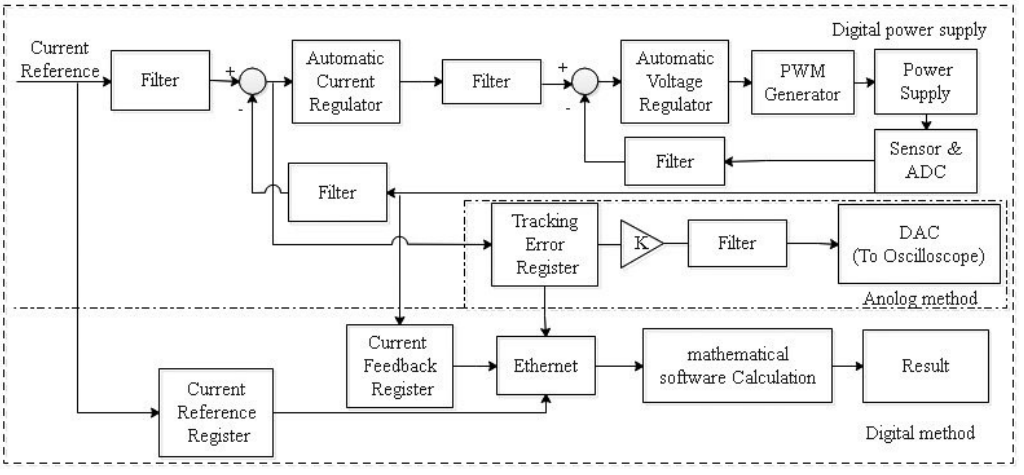

Fig. 2. Tracking error measurement methods of digital pulse power supplies.

approximate evaluation. The digital method does not require additional cost and only the digital regulator hardware. The tracking error can be calculated quantitatively using the digital method without any errors resulting from visual measurement. Moreover, various types of data can be effectively sampled and analysed using the digital method, allowing optimization of regulator parameters.

4. Traditional tracking error reconstruction method

In an accelerator system, the transmission and collection of pulse power supply tracking error can easily be disturbed. Accordingly, it is necessary to reconstruct the acquired signal before it is used as the index to estimate the power supply performance. There are two methods of traditional tracking error reconstruction, described in detail below.

4.1. Frequency domain filtering

In digital methods, it is the most important to filter the noise interference for the sampled signal reconstruction. The targeted signal of the heavy ion accelerator power supply is 1 kHz, which means the filter should not work on signals below 1 kHz. The Butterworth filter indicates that signal under 1 kHz is within the pass band range, but there is a phase shift problem after filtering. This method does not allow effective theoretical support for signal-noise separation of any selected band frequency, and because of the smearing of the filter, it is difficult to remove all interference signals.

4.2. Wavelet threshold de-noising

For time-frequency analysis, wavelet transform methods have great advantages when compared to Fourier transform methods and are better than traditional frequency domain filtering methods for tracking error reconstruction in a pulse power supply system. At present, wavelet de-noising is based on a threshold de-noising algorithm, and its basic steps are as follows [12, 13]:

1. Setting appropriate wavelet basis function and decomposition level and, then, the high frequency and low frequency wavelet coefficients can be obtained by wavelet transform.
2. After selecting the threshold parameter and threshold function, threshold de-noising is performed on the high frequency wavelet coefficients, and the soft threshold function is selected as the de-noise platform, which is as follows:

$$W_T = \begin{cases} \text{sign}\,(W) * (|W| - T) & |W| \geq T \\ 0 & |W| < T \end{cases}, \tag{3}$$

   where the threshold parameter is $T = \sigma\sqrt{2\log N}$, W is the wavelet coefficient, σ is the standard deviation of noise, and N is the signal length.
3. The low frequency wavelet coefficients and the high frequency wavelet coefficients are used for inverse transformation and reconstruction to obtain the de-noising signal.

Practically, wavelet threshold de-noising is restricted by both the threshold parameter and selection of the function with no adaptability.

Metrol. Meas. Syst., Vol. 27 (2020), No. 2, pp. 339–353
DOI: 10.24425/mms.2020.132779

5. Tracking error reconstruction method based on empirical mode decomposition

5.1. Principle of empirical mode decomposition

EMD uses the time scale characteristics of the signal itself to decompose the signal. It is an adaptive process, and is fundamentally different from the Fourier decomposition and wavelet decomposition methods. The frequencies of the *intrinsic mode functions* (IMFs) decomposed by the EMD are then arranged from high to low for signal reconstruction, where each IMF is a single component with only a single frequency. EMD can theoretically be applied to the decomposition of any type of signal, providing an obvious advantage for the analysis of non-stationary and nonlinear data, with a high signal to noise ratio. It is a process of decomposing and sifting, and the decomposed IMFs must meet two conditions:

1. The difference in number between extreme points and zero points of the signal is at most one.
2. The local mean value of the upper and lower envelopes fitted by the maximum and minimum values of the signal is zero.

The decomposition process of EMD is as follows [14-19]:

1. $x(t)$ is the original signal and $n = n + 1$ represents the time of decomposition (the initial value is 0).
2. Calculate the extreme value of the signal $y(t)$ and $y(t) = x(t)$.
3. Calculate the envelopes $(up(t), down(t))$ with cubic spline and calculate the average of the envelopes, that is $m(t) = (up(t), down(t))/2$.
4. If $h(t) = y(t) - m(t)$ meets the characteristics of IMF, then $h(t)$ is the n-th IMF (IMF_n) so can proceed to the next step. If not, then the signal $y(t)$ is replaced by $h(t)$ and it is necessary to return to step 2.
5. If $r(t) = x(t) - h(t)$ is monotonous or there is only one extreme point, then the decomposition of EMD ends, and n is the number of IMF components. If not, then the signal of decomposition is replaced by $r(t)$ and it is necessary to return to step 1.

The result of the decomposition should satisfy the following formula [20, 21]:

$$x(t) = \sum_{i=1}^{n} IMF_i(t) + r(t), \tag{4}$$

where $x(t)$ is the original signal, $IMF_i(t)$ are components of EMD, and $r(t)$ is the residue component. Since the decomposition of EMD satisfies completeness, it is possible to reconstruct the original signal accurately by using all of the components.

5.2. Boundary problem

Cubic spline interpolation is used to calculate envelopes based on local extreme points in EMD. It is cannot determine extreme points effectively at both ends of the signal for its finite length which causes envelopes distortion at ends, and this phenomenon is defined boundary problem [22–24].

To solve the boundary problem, this paper uses extreme point symmetric extension. Left and right extension are symmetric and take left extension as an example. Figure 3 shows the extension under different symmetry points. The signal, maximum and minimum sequences are $\{x(1), x(2), \ldots, x(N)\}$, $\{x(m_1), x(m_2), \ldots, x(m_m)\}$ and $\{x(n_1), x(n_2), \ldots, x(n_n)\}$, where $m_m < N$, $n_n < N$. When $m_1 < n_1$ and $x(1) > x(n_1)$, the symmetry point is $(m_1, x(m_1))$ as shown in Fig. 3a.

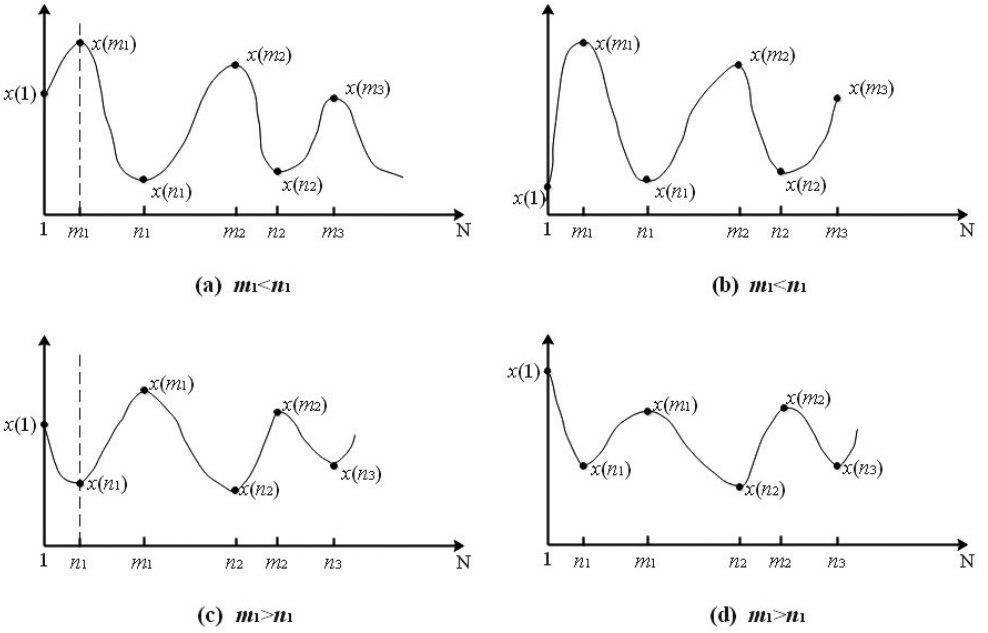

Fig. 3. Extreme points left extension under different symmetry points.

Figure 3b presents that $(1, x(1))$ is the symmetry point if $m_1 < n_1$ and $x(1) < x(n_1)$. Under $n_1 < m_1$, choose $(n_1, x(n_1))$ as the symmetry point when $x(1)$ and $x(m_1)$ satisfy the condition $x(1) < x(m_1)$ elaborated in Fig. 3c, otherwise select $(1, x(1))$ which is given in Fig. 3d.

5.3. Mode mixing

Mode mixing refers to the phenomenon that there are different characteristic scales in an IMF, or similar characteristic scales are dispersed in different IMFs. To solve mode mixing, N.E. Huang proposed *Ensemble Empirical Mode Decomposition* (EEMD) [25]. Using the uniform distribution of white noise in the time-frequency spectrum, EEMD adds white noise to the original signal. But the method has the white noise residual and causes illusive components. Reference [26] locates the discontinuous signal by using frequency characteristics of IMF and redone EMD to separate the discontinuous signal segment. The location, however, requires empirical judgment.

This paper uses a novel method to solve mode mixing proposed by Robertas Damaševičius. The method adds a set post-processing stage for adjacent IMFs as follows: remixing, EMD, splitting, and de-mixing. The splitting is performed by finding a cut in the set of IMFs that provides the smallest correlation between the sum of IMFs with higher frequency and the sum of IMFs with lower frequency as follows:

$$\arg\min_{1<k<n} corr \sum_{1\le i\le k} IMF_l, \sum_{k\le i\le n} IMF_l, \tag{5}$$

where n is the number of IMFs derived from the signal.

Metrol. Meas. Syst., Vol. 27 (2020), No. 2, pp. 339–353
DOI: 10.24425/mms.2020.132779

5.4. Filtering characteristics of EMD

The complex signal is decomposed into IMF components $IMF_{1\sim n+1}$ by EMD, and the frequency distribution of the individual components can be arranged from high to low. Next, the residue component $r(t)$ is evaluated as the IMF component, and different filters can be applied as follows [27]:

$$x'(t) = \sum_{l}^{h} IMF_l(t) \qquad (1 \le l \le h \le n+1), \tag{6}$$

$$\begin{aligned} &l > 1 \text{ and } h = n+1, && \text{is a low-pass filter,}\\ &l = 1 \text{ and } h < n+1, && \text{is a high-pass filter,}\\ &l > 1 \text{ and } h < n+1, && \text{is a band-pass filter.} \end{aligned}$$

The instantaneous frequency of each IMF component can be obtained by Hilbert transform (HT). The cutoff frequency is used to filter out some IMF components of unwanted frequency, giving surplus IMF components. In this way, this process serves as an adaptive filter.

5.5. EMD reconstruction method

The tracking error of current in the digital pulse power supply can be disturbed by white noise. The mathematical model can be expressed as:

$$x(t) = n(t) + noise\,(t), \tag{7}$$

where $noise\,(t)$ is Gaussian white noise, of which the variance is σ^2. $n(t)$ is the original signal. The EMD result of $x(t)$ can be expressed as formula (4), and the noise and useful information should always be included in each order component. The components for which the noise is greater than the useful information are considered noise-dominated components, and the other components are called signal-dominated components [28, 29]. Accordingly, the key of reconstruction is identification of the noise and the signal-dominated components.

Reference [30] proposes a feature extraction and selection method of signals based on energy spectrum of IMFs. IMFs are transformed into energy spectrum feature vectors and then Support Vector Machine is used to classify them to achieve identification of IMF components. However, this method requires off-line training and has limitations of the sample. Reference [31] proposes an EMD de-noising method based on Singular Spectrum Analysis (SSA), which removes the first IMF component and the noise parts of other IMF components by singular value decomposition reconstruction. But the principle component selection of SSA is empirical. Reference [32] directly applies the wavelet threshold de-noising theory to the EMD de-noising method. Nevertheless, the wavelet de-noising object is the wavelet coefficient, while the EMD de-noising object is the sampled data.

During the EMD de-noising to the tracking error in this paper, the threshold de-noising process of the noise-dominated components is neglected, because the de-noising result is not obviously enhanced relative to the reconstruction of only the signal-dominated components. After original signal decomposition, the energy of the noise-dominated components exhibits a decreasing trend. However, the energy increases after the attenuation of the noise energy has decreased to the lowest value because after this IMF_k, the components begin to be dominated by the signal [33, 34]. The order k that corresponds to the first local minimum of energy can be used as the critical order,

and the next order component is the signal-dominated one. The energy formula of each order is expressed as follows:

$$E_i = \sum_{j=1}^{N} IMF_i^2(t) \quad i = 1, 2, 3, \ldots, n{+}1, \tag{8}$$

where E_i is the energy of the i-th component, $n{+}1$ is the decomposition order, and N is the sequence length.

6. Verification and experiment

The output current sampled from the pulse power supply contains a lot of noise, making it difficult to directly obtain the current tracking error. This section presents both theoretical and experimental validation of the EMD method for the tracking error reconstruction of signal from a pulse power supply. First, the reference current plus Gaussian white noise is used to simulate actual sampled signal from a pulse power supply. Then, the signal is reconstructed by the de-noising algorithm described above, and the *signal-to-noise ratio* (SNR) and *root-mean-square error* (RMSE) are compared as aspects of the de-noising performance. Second, the real output current signal from a pulse power supply prototype is reconstructed, and the tracking error is calculated and analysed.

6.1. Theoretical verification

SNR and RMSE are calculated to evaluate the de-noising performance, and a larger SNR value and smaller RMSE value correspond to better de-noising performance. The calculation formulas are as follows:

$$\mathrm{SNR} = 10 \log \frac{\sum_{i=1}^{N} n^2(t)}{\sum_{i=1}^{N} \left[n(t) - y(t)\right]^2}, \tag{9}$$

$$\mathrm{RMSE} = \sqrt{\frac{\sum_{i=1}^{N} \left[n(t) - y(t)\right]^2}{N}}, \tag{10}$$

where $n(t)$ and $y(t)$ are the original and de-noised signal respectively.

The Gaussian white noise with $\sigma = 0.001$ and $\sigma = 0.035$ is respectively added to the flat-top stage and rising stage of the reference current waveform to simulate the actual sampled output current of the pulse power supply. EMD is then applied to decompose the signal, allowing identification of its energy turning point and reconstruction of the useful signal. Taking the rising stage as an example, 17 components are obtained by decomposition of the signal from the rising stage. The turning point of the energy as calculated by the energy formula is the ninth component, and the signal-dominated components $IMF_{10\sim17}$ are reconstructed to obtain a de-noising signal.

Considering the size limitation of figures, Fig. 4 only shows the first two and last components of noise-dominated IMF, and it shows the reconstruction of the signal as well. As can be seen from Fig. 5, the first local minimum point in the energy graph is the 9-th order, so the components

www.czasopisma.pan.pl PAN POLSKA AKADEMIA NAUK www.journals.pan.pl
Metrol. Meas. Syst., Vol. 27 (2020), No. 2, pp. 339–353
DOI: 10.24425/mms.2020.132779

after the 9-th order are then reconstructed as the de-noised signal. The reconstructed result is shown in Fig. 4.

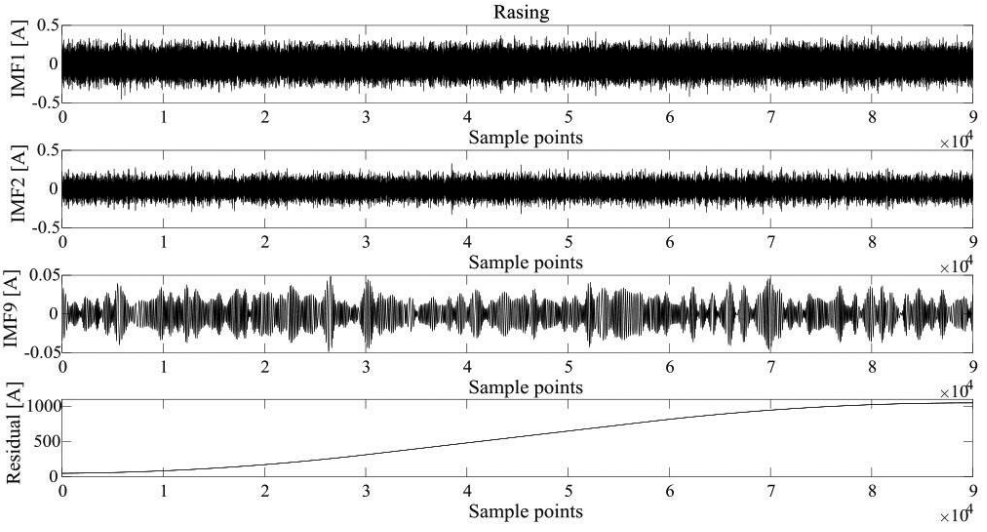

Fig. 4. 1st, 2nd and 9th order IMF and reconstructed signal.

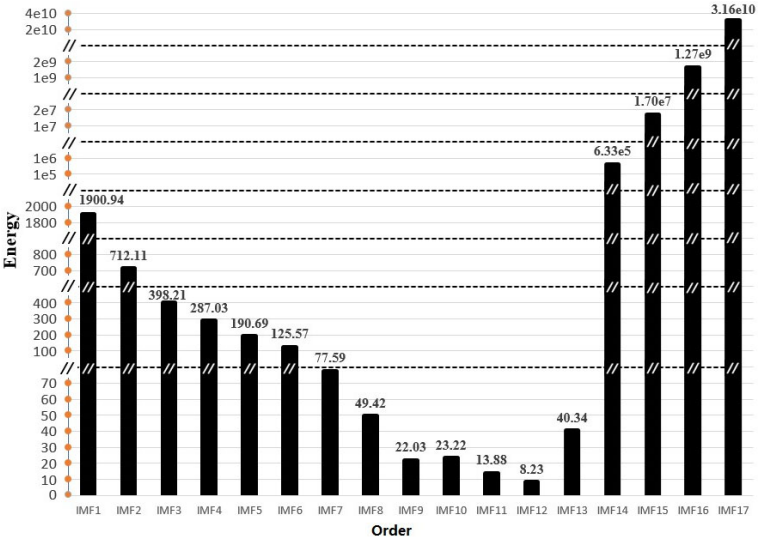

Fig. 5. Energy trend chart of the rising stage.

To compare the reconstruction methods, the simulated signal is de-noised using the frequency domain, the wavelet threshold, and the EMD methods. The current tracking error is obtained by removing the reference current from the de-noising signal, as shown in Fig. 5.

As shown in Fig. 6, the tracking error of the original signal on rising stage is about ±0.5 A and that of the flat-top stage is ±0.1 A. The de-noising results show that EMD is superior to the

other two methods in all stages of the pulse waveform. Specifically, the relative tracking error in the rising stage is within $\pm 5.0 \times 10^{-5}$ and that in the flat-top stage is within $\pm 1.0 \times 10^{-5}$. Both values meet the de-noising requirements of the current tracking error in the accelerator pulse power supply system. The results of three de-noising algorithms are presented in Tables 2 and 3.

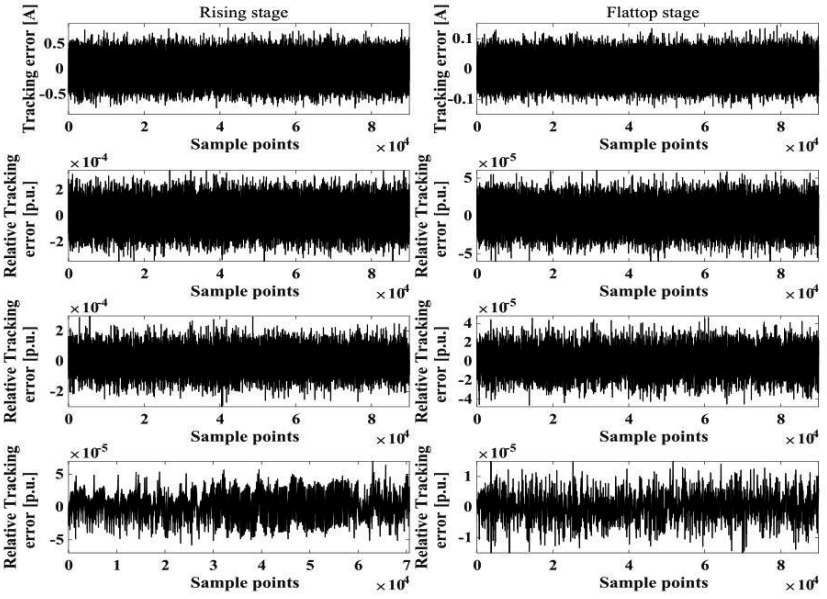

Fig. 6. Original signal and de-noising results of the three reconstruction methods (from top to bottom: original signal, frequency domain filtering, wavelet threshold de-noising, EMD reconstruction).

Table 2. Performance of three reconstruction methods in the rising stage.

Performance	Original signal $x(t)$	Butterworth	Wavelet	EMD
SNR (dB)	70.4	76.7	79.4	92.2
RMSE	0.200	0.097	0.071	0.016

Table 3. Performance of three reconstruction methods in the flat-top stage.

Performance	Original signal $x(t)$	Butterworth	Wavelet	EMD
SNR (dB)	90.0	96.3	99.0	107.0
RMSE	0.033	0.0161	0.0118	0.0047

In the accelerator pulse power supply system shown in Table 1, using the dipolar magnet power supply as an example, the relative tracking error in the rising stage should be within $\pm 1.0 \times 10^{-4}$ and that in the flat-top stage should be within $\pm 1.0 \times 10^{-5}$. If the simulated tracking error signal meets the requirements of Table 1 for dipolar magnet power supplies, then according to formula (9), the result of the de-noising algorithm should reach 80 dB in the rising stage and 100 dB in the flat-top stage. The data in Tables 2 and 3 show that the EMD result not only meets these requirements but provides the maximum SNR and minimum RMSE values of the three methods.

Metrol. Meas. Syst., Vol. 27 (2020), No. 2, pp. 339–353
DOI: 10.24425/mms.2020.132779

As described above, the EMD method does not depend on basis function or the selection of decomposition level, as this process is adaptive during de-noising. Additionally, there is no phase shift problem arising from frequency domain filtering. Therefore, this is seems to be the best approach to reconstruct and analyse the tracking error of a pulse power supply.

6.2. Experiment and analysis of prototype

This approach is tested experimentally using a power supply prototype that excites a dipolar magnet in HIMM, and its parameters are shown in Table 4 [2]. A pulse waveform is chosen as the reference current, with a rise time of 1 s and 1050 A current in the flat-top stage. The digital regulator of the prototype can synchronously sample the reference and output feedback using a sampling frequency of 62.5 kHz. The output current and tracking error of the pulse power supply are shown in Fig. 7. In order to facilitate the analysis and observation of the tracking error, 90, 000 data points were selected for analysis in the flat-top stage and in the rising stage. Accurate tracking is required in the rising stage, while rapid tracking is the sought performance in the flat-top stage, which cannot be both achieved by the digital regulator at the same time. Therefore, when controlling the digital regulator, to meet the current requirements in the flat-top stage, the regulator must function on a slight overshooting state to achieve fast tracking performance in the current rises. The relative error range after de-noising by the three algorithms is shown in Table 5.

Table 4. Parameters of the power supply prototype.

Type	Value	Type	Value
Load resistance	53.3 mΩ	Relative tracking error [p.u.]	$\leq \pm 1.0 \times 10^{-4}$
Load inductor	106 mH	Relative current error [p.u.]	$\leq \pm 1.0 \times 10^{-5}$
Maximum current	1150 A	Rise time	1 s
Maximum voltage	185 V	Ripple current	≤ 0.025 A

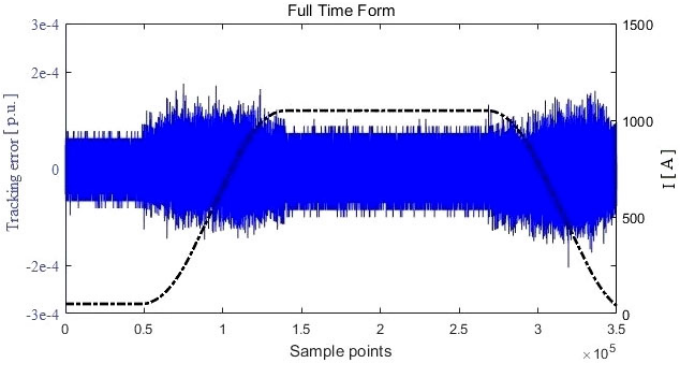

Fig. 7. Output current and tracking error of the pulse power supply.

Because of sampled noise, the relative current tracking error in the rising stage is approximately $\pm 1.5 \times 10^{-4}$ and that in the flat-top stage is about $(-0.8 \pm 9.2) \times 10^{-5}$, insufficient to meet the design requirements and not representative of the tracking performance of the power supply. After reconstruction, the relative tracking errors calculated by the three de-noising algorithms is

Table 5. The relative error range for the pulse power supply prototype.

Stage	Original signal [p.u.]	Frequency domain filtering [p.u.]	Wavelet threshold denoising [p.u.]	EMD reconstruction [p.u.]
Rising	$\pm 1.5 \times 10^{-4}$	$\pm 1.0 \times 10^{-4}$	$\pm 1.0 \times 10^{-4}$	$\pm 0.8 \times 10^{-4}$
Flat-top	$(-0.8 \pm 9.2) \times 10^{-5}$	$(-0.8 \pm 2.8) \times 10^{-5}$	$(-0.8 \pm 2) \times 10^{-5}$	$(-0.8 \pm 0.8) \times 10^{-5}$

all within the index range of the power supply. The relative tracking error of the EMD de-noising algorithm in the rising stage is about $\pm 0.8 \times 10^{-4}$. The relative tracking error range in flat-top stage is about $(-0.8 \pm 0.8) \times 10^{-5}$, which meets the fact. But it is not obvious in frequency domain filtering or the wavelet threshold algorithm. The waveform of the flat-top stage is shown in Fig. 8.

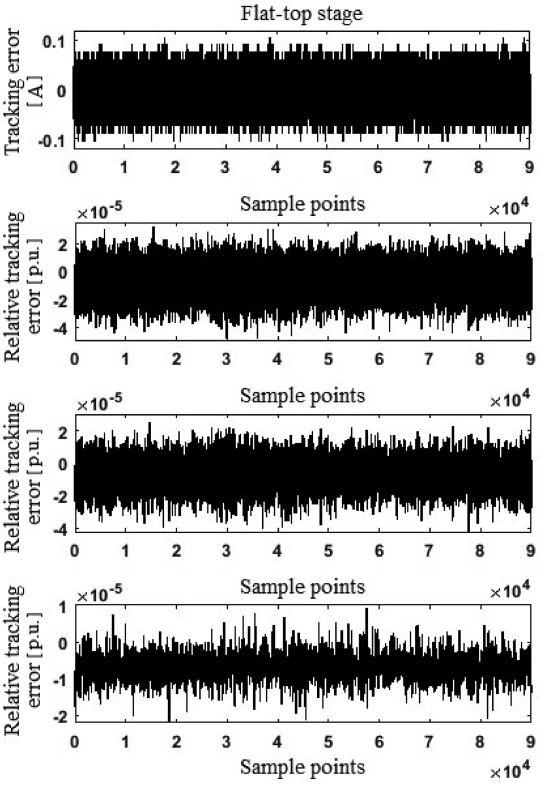

Fig. 8. Tracking error and reconstruction result of flat-top stage (from top to bottom: original signal, frequency domain filtering, wavelet threshold de-noising, EMD reconstruction).

The results from the experiments and simulations show significant noise in the signal after frequency domain filtering and application of the wavelet threshold algorithm. The EMD method better filters the noise, retains the tracking error information, and also shows the details of true signals that were hidden in the noise. Overall, this method effectively characterizes true power supply performance, providing data that can be used to guide power control strategy and facilitate parameter optimization.

7. Conclusions

This paper proposes a threshold de-noising method based on EMD. The turning point of energy of IMF components is identified by the proposed method. To achieve good performance, this paper proposes a method of extreme point symmetric extension to solve the boundary problem and uses a novel method to solve mode mixing. And then an adaptive low-pass filter is designed by using the characteristics of EMD, which is used to filter the noise-dominated IMF components. A comparison of the proposed reconstruction algorithm with the traditional de-noising methods shows that the proposed approach has better SNR and adaptability. The data filtering facilitates the tuning of operational parameters. The filtering algorithm can also be added to the feedback channel for better tracking. This method allows the decomposition of sampled signals and energy analysis of IMFs to reconstruct signal-dominated components. Future work should address methods for further de-noising to extract useful from noise-dominated components for more accurate assessment.

Acknowledgements

This research was supported by Institute of Modern Physics, Chinese Academy of Sciences. The authors thank the Institute for providing the power supply prototype and experimental environments. This work is supported by the National Natural Science Foundation of China [grant number 51707068], the Natural Science Foundation of Fujian Province [grant number 2017J01097].

References

[1] Wu, F., Gao, D., Shi, C., Huang, Y., Cui, Y., Yan, H., Zhang, H., Wang, B., Li X. (2016). A new type of accelerator power supply based on voltage-type space vector PWM rectification technology. *Nuclear Instruments & Methods in Physics Research Section A*, 826, 1–5.

[2] Wang, R., *et al.* (2013). A new digital pulse power supply in heavy ion research facility in Lanzhou. *Nuclear Instruments & Methods in Physics Research Section A*, 727, 46–50.

[3] Zhao, J., *et al.* (2015). Implementation of an FPGA controller for correction power supplies in heavy ion synchrotron. *Nuclear Instruments & Methods in Physics Research Section A*, 777, 167–171.

[4] Wang, R., *et al.* (2013). Synchronization Method of Digital Pulse Power Supply for Heavy Ions Accelerator in Lanzhou. *Atomic Energy Science & Technology*, 47(4), 683–686 (in Chinese).

[5] Borkowski, D. (2018). An Improved Method of Busbar Voltage Reconstruction from Signals of Electric Field Sensors Installed in an Indoor MV Substation. *Metrology and Measurement Systems*, 25(1), 71–86.

[6] Wang, F., Yu, N. (2017). An Ultracompact Butterworth Low-Pass Filter Based on Coaxial Through-Silicon Vias. *IEEE Transactions on Very Large Scale Integration (VLSI) Systems*, 25(3), 1164–1167.

[7] Hilton, M.L., Ogden, R.T. (1997). Data analytic wavelet threshold selection in 2-D signal denoising. *IEEE Transactions on Signal Processing*, 45(2), 496–500.

[8] Smith, C.B., Agaian, S., Akopian, D. (2008). A Wavelet-Denoising Approach Using Polynomial Threshold Operators. *IEEE Signal Processing Letters*, 15, 906–909.

[9] Prucnal, M., Polak, A.G. (2017). Effect of Feature Extraction on Automatic Sleep Stage Classification by Artificial Neural Network. *Metrology and Measurement Systems*, 24(2), 229–240.

[10] Yan, H., Gao, D., Zhou, Z., Wang, J. (2010). Research on the Test Method of Tracking Error for Pulse Switching Power Supply. *Power Supply Technologies & Applications*, 13(2), 9–11 (in Chinese).

[11] Wang, R. (2013). *Research and design of dedicated digital power supply regulator for medical heavy ion accelerator*. Ph.D. Thesis. University of Chinese Academy of Sciences (in Chinese).

[12] Donoho, D.L. (1995). De-noising by soft-thresholding. *IEEE Transactions on Information Theory*, 41(3), 613–627.

[13] Ching, P.C., So, H.C., Wu, S.Q. (1999). On wavelet denoising and its applications to time delay estimation. *IEEE Transactions on Signal Processing*, 47(10), 2879–2882.

[14] Hu, X., Peng, S., Hwang, W.-L. (2012). EMD Revisited: A New Understanding of the Envelope and Resolving the Mode-Mixing Problem in AM-FM Signals. *IEEE Transactions on Signal Processing*, 60(3), 1075–1086.

[15] Huang, N. E., Wu, Z. (2008). A review on Hilbert-Huang transform: Method and its applications to geophysical studies. *Reviews of Geophysics*, 46(2), 1–23.

[16] Boudraa, A.-O., Cexus, J.-C. (2007). EMD-Based Signal Filtering. *IEEE Transactions on Instrumentation & Measurement*, 56(6), 2196–2202.

[17] Rilling, G., Flandrin, P. (2008). One or Two Frequencies? The Empirical Mode Decomposition Answers. *IEEE Transactions on Signal Processing*, 56(1), 85–95.

[18] Yaslan, Y., Bican, B. (2017). Empirical mode decomposition based denoising method with support vector regression for time series prediction: A case study for electricity load forecasting. *Measurement*, 103, 52–61.

[19] Wang, R., Sun, S., Guo, X., Yan, D. (2018). EMD Threshold Denoising Algorithm Based on Variance Estimation. *Circuits Systems & Signal Processing*, 37(12), 5369–5388.

[20] Lu, S., Wang, X., Yu, H., Dong, H., Yang, Z. (2017). Trend extraction and identification method of cement burning zone flame temperature based on EMD and least square. *Measurement*, 111, 208–215.

[21] Khaldi, K., Boudraa, A O. (2012). On signals compression by EMD. *Electronics Letters*, 48(21), 1329–1331.

[22] Li, S., Li, H., Ma, L. (2013). A Real Signal Model-Based Method for Processing Boundary Effect in Empirical Mode Decomposition. *2013 Third International Conference on Instrumentation, Measurement, Computer, Communication and Control*, Shenyang, China.

[23] Deng, Y., Wang, W., Qian, C., Wang, Z., Dai, D. (2001). Boundary-processing-technique in EMD method and Hilbert transform. *Chinese Science Bulletin*, 46(1), 954–960.

[24] Zeng, K., He, M. (2004). A simple boundary process technique for empirical mode decomposition. *2004 IEEE International Geoscience and Remote Sensing Symposium (IGARSS 2004)*, Anchorage, AK, USA.

[25] Wu, Z., Huang, N.E. (2009). Ensemble empirical mode decomposition: a noise assisted data analysis method. *Advances in Adaptive Data Analysis*, 1(1), 1–41.

[26] Damasevicius, R., Napoli, C., Sidekerskiene, T., Wozniak, M. (2017). IMF mode demixing in EMD for jitter analysis. *Journal of Computational Science*, 22, 240–252.

[27] Flandrin, P., Rilling, G., Goncalves, P. (2004). Empirical mode decomposition as a filter bank. *IEEE Signal Processing Letters*, 11(2), 112–114.

[28] Li, H., Wang, X., Chen, L., Li, E. (2014). Denoising and R-Peak Detection of Electrocardiogram Signal Based on EMD and Improved Approximate Envelope. *Circuits Systems & Signal Processing*, 33(4), 1261–1276.

Metrol. Meas. Syst., Vol. 27 (2020), No. 2, pp. 339–353
DOI: 10.24425/mms.2020.132779

[29] Li, M., Wu, X., Liu, X. (2015). An Improved EMD Method for Time–Frequency Feature Extraction of Telemetry Vibration Signal Based on Multi-Scale Median Filtering. *Circuits Systems & Signal Processing*, 34(3), 815–830.

[30] Li, S., Zhou, W., Yuan, Q., *et al.* (2013). Feature extraction and recognition of ictal EEG using EMD and SVM. *Computers in Biology & Medicine*, 43(7), 807–816.

[31] Lu, Y., Saniie, J. (2016). A comparative study of singular spectrum analysis and empirical mode decomposition for ultrasonic NDE. *2016 IEEE International Ultrasonics Symposium (IUS)*, Tours, France.

[32] Boudraa, A.-O., Cexus, J.-C. (2006). Denoising via empirical mode decomposition. *Proc. of Second International Symposium on Communications, Control and Signal Processing (ISCCSP 2006)*, Marrakesh, Morocco.

[33] Zhu, S., Liu, L., Yao, Z. (2018). The application of threshold empirical mode decomposition de-noising algorithm for battlefield ambient noise. *International Journal of Modeling, Simulation, and Scientific Computing*, 9(4), 1850027.

[34] Che, L., Di, Y., Gu, X., *et al.* (2017). A signal de-noising method for gas switch discharge based on EMD and energy ratio. *2017 IEEE 2nd Advanced Information Technology, Electronic and Automation Control Conference (IAEAC)*, Chongqing, China.